

Improved method for measuring photoacid generator kinetics in polymer thin films using normalized interdigitated electrode capacitance data

Cody M. Berger and Clifford L. Henderson

Citation: *J. Vac. Sci. Technol. B* **22**, 1163 (2004); doi: 10.1116/1.1755219

View online: <http://dx.doi.org/10.1116/1.1755219>

View Table of Contents: <http://avspublications.org/resource/1/JVTBD9/v22/i3>

Published by the AVS: Science & Technology of Materials, Interfaces, and Processing

Additional information on *J. Vac. Sci. Technol. B*

Journal Homepage: <http://avspublications.org/jvstb>

Journal Information: http://avspublications.org/jvstb/about/about_the_journal


Top downloads: http://avspublications.org/jvstb/top_20_most_downloaded

Information for Authors: http://avspublications.org/jvstb/authors/information_for_contributors

ADVERTISEMENT

Instruments for advanced science

Gas Analysis




- dynamic measurement of reaction gas streams
- catalysis and thermal analysis
- molecular beam studies
- dissolved species probes
- fermentation, environmental and ecological studies

Surface Science




- UHV TPD
- SIMS
- end point detection in ion beam etch
- elemental imaging - surface mapping

Plasma Diagnostics



- plasma source characterization
- etch and deposition process reaction kinetic studies
- analysis of neutral and radical species

Vacuum Analysis



- partial pressure measurement and control of process gases
- reactive sputter process control
- vacuum diagnostics
- vacuum coating process monitoring

contact Hiden Analytical for further details

HIDEN

ANALYTICAL

info@hideninc.com

www.HidenAnalytical.com

CLICK to view our product catalogue

Improved method for measuring photoacid generator kinetics in polymer thin films using normalized interdigitated electrode capacitance data

Cody M. Berger and Clifford L. Henderson^{a)}

School of Chemical & Biomolecular Engineering, Georgia Institute of Technology 311 Ferst Drive, Atlanta, Georgia 30332-0100

(Received 11 July 2003; accepted 5 April 2004; published 24 May 2004)

A data analysis method is presented that can be used to calculate kinetic rate constants for photoacid generation (Dill C values) in polymer and chemically amplified photoresist thin films using capacitance versus exposure dose data from resist coated interdigitated electrode (IDE) sensors. It is shown that the use of normalized IDE capacitance data can reduce or eliminate errors and variations in measured Dill C values obtained from our previous analysis method that are created by environmental factors such as humidity fluctuations and IDE factors such as variations in electrode geometry and size. Using this normalization method, the Dill C rate constants for 248 nm exposure of triphenylsulfonium triflate (TPS–Tf), triphenylsulfonium perfluoro-1-butanesulfonate (TPS–Nf), bis(4-tert-butylphenyl)iodonium triflate (TBI–Tf), and bis(4-tert-butylphenyl)iodonium perfluoro-1-butanesulfonate (TBI–Nf) in poly(p-hydroxystyrene) (PHOST) were found to be 0.046, 0.040, 0.055, and 0.056 cm²/mJ, respectively. These results are shown to compare well with values obtained for these same systems using our original IDE data analysis method (0.045 cm²/mJ for TPS–Tf/PHOST, 0.039 cm²/mJ for TPS–Nf/PHOST, 0.056 cm²/mJ for TBI–Tf/PHOST, and 0.054 cm²/mJ for TBI–Nf/PHOST). The normalization method has a significant advantage in that it permits the determination of a Dill C parameter for a particular polymer-photoacid generator system using a single resist film coated IDE and a single exposure experiment. © 2004 American Vacuum Society. [DOI: 10.1116/1.1755219]

I. INTRODUCTION

Chemically amplified photoresists have been the lithographic imaging material of choice for high resolution patterning in the semiconductor industry now for over a decade, and will likely see continued use for many years to come. With such widespread use, the ability to fully understand the lithographic behavior of chemically amplified photoresists is a critical tool for both enabling improvements in existing photolithography processes and materials and the development of materials and processes for the future generations of devices. One of the first issues that must be understood and quantified in characterizing chemically amplified photoresist behavior is the rate of photoacid generation from the photoacid generators (PAGs) used in such materials.

Positive-tone chemically amplified photoresists rely on a two-step mechanism to achieve imaging in the resist film.¹ First, exposure to ultraviolet (UV) radiation causes a PAG to decompose and produce an acid within the film. Second, the photogenerated acid then catalyzes a thermal deprotection reaction that renders the resist matrix polymer soluble in an aqueous developer. Figure 1 illustrates a representative exposure and deprotection process for a triphenylsulfonium triflate PAG in a tetrahydropyranyl ether protected poly(p-hydroxystyrene) (PHOST) matrix.¹

Photogenerated acid is directly responsible for activating the solubility switching mechanism in chemically amplified photoresists, and hence, the imaging capabilities of the resist

depend strongly on the process of acid generation, diffusion, and reaction. Therefore, one of the first and most critical steps in understanding and potentially modeling the lithographic behavior of a chemically amplified photoresist is determining the amount and rate at which acid is generated within the resist film. Recently the development of a technique for measuring the kinetics of photoacid generation in resist films was reported.^{2,3} This technique utilizes capacitance measurements of resist coated interdigitated (IDE) electrodes to measure the kinetic rate constant for photoacid generation, often referred to as the Dill C parameter. In this method, a thin polymer film loaded with a PAG is spin coated onto an IDE and a base line capacitance measurement is recorded. The resist film is then exposed to a small dose of UV radiation which results in some photoreaction of the PAG and the production of a small amount of photoacid. Since the decomposition products of the PAG possess different dielectric properties than the initial PAG molecule, the net dielectric constant of the polymer film will change and result in a measurable change in IDE capacitance. By properly analyzing the changes measured in capacitance during exposure, it is possible to extract the Dill C parameter.

This article discusses a recent advancement in this Dill C measurement routine that involves a technique for normalizing the raw capacitance data that is collected from the IDE and performing the resulting kinetics analysis using this normalized data set. Performing subsequent analysis using this normalized data set offers a number of advantages over the original method which involved analysis of the raw capacitance data. First, the normalization technique allows for im-

^{a)}Author to whom correspondence should be addressed; electronic mail: cliff.henderson@chbe.gatech.edu

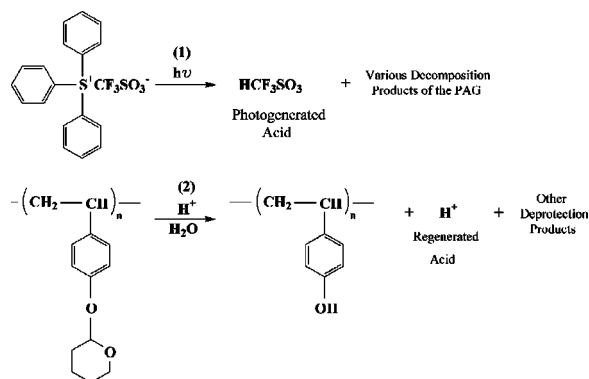


FIG. 1. Exposure (1) of TPS-Tf PAG and acid catalyzed deprotection (2) of tetrahydropyranyl ether protected PHOST.

proved accuracy in the Dill C values calculated from the raw data of different IDE sensor experiments by eliminating sensor to sensor variations caused by factors such as slight variations in electrode geometry or baseline electrical properties and by eliminating the effects of changing laboratory conditions such as relative humidity. In addition, the normalization technique discussed makes it possible in theory to measure the Dill C parameter for a photoacid generator with the data collected from a single IDE, as opposed to the multiple IDE experiments discussed in our previous work.^{2,3} This ability to use a single IDE sensor measurement can substantially reduce the time required for experiments and reduce the use of potentially rare and expensive materials. Finally, the normalization technique proposed in this article could make it possible to determine the Dill C parameter for a photoacid generator in a resist whose composition and PAG loadings are completely unknown. This last advantage of permitting experiments on “unknown” samples could prove to be potentially very powerful for characterizing commercial photoresist materials where the composition of such materials tends to be a closely guarded secret.

II. EXPERIMENT

A. Materials and sample preparation

Electronic grade poly(p-hydroxystyrene) ($M_w = 11\,800$) was obtained from Triquest Chemical Company and used as the matrix polymer for all experiments. Triphenylsulfonium triflate (TPS-Tf), triphenylsulfonium perfluoro-1-butanesulfonate (TPS-Nf), bis(4-tert-butylphenyl)iodonium triflate (TBI-Tf), and bis(4-tert-butylphenyl)iodonium perfluoro-1-butanesulfonate (TBI-Nf) were used as the photoacid generators (Sigma Aldrich) while ethyl lactate (Sigma Aldrich, 98%) was used as the casting solvent for all solutions used in this work. The polymer, PAGs, and solvent were all used as received. Figure 2 illustrates the structure of both the PHOST matrix and the PAGs used in this work.

The PHOST matrix and PAGs were mixed to create solutions ranging from 13 to 15 wt % solids, with PAG loadings ranging from 0 to 5 wt % by solids. All solutions were filtered through 0.2 μm Teflon filters and spin coated at 900 rpm for 30 s onto interdigitated electrode structures (de-

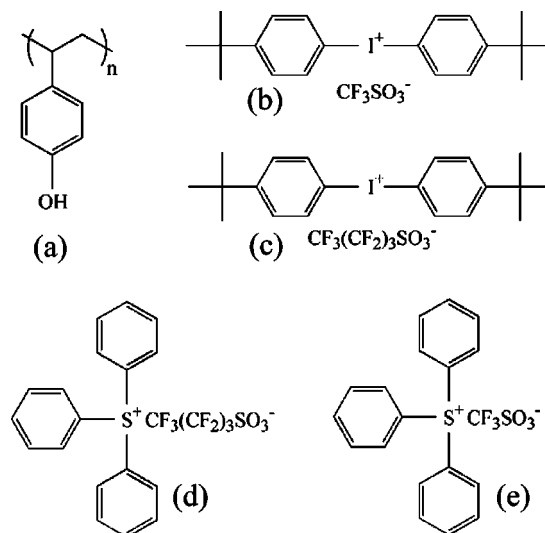


FIG. 2. Chemical structures of (a) PHOST, (b) TBI-Tf, (c) TBI-Nf, (d) TPS-Tf, and (e) TPS-Nf.

scribed later) using a CEE model 100 CB spin coat and bake system (Cost Effective Equipment). These spin coat and bake conditions resulted in films approximately 1.5 μm in thickness. A contact hotplate soft bake at 115 $^{\circ}\text{C}$ for 1 min was performed after spin coating to remove residual casting solvent from the films.

B. Interdigitated electrode structures

In this work, IDE structures were used to characterize the dielectric response of polymer thin films to reactions occurring within the film. The geometry of the IDE structures used in this work is illustrated in Fig. 3. As shown in the figure, the interdigitated electrodes used in these experiments consisted of interdigitated aluminum electrode fingers and bond pads deposited on top of an insulating layer of silicon dioxide, all residing on a silicon substrate. The entire length of

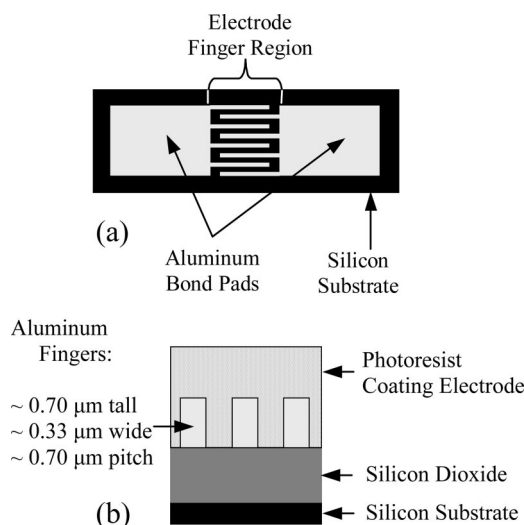


FIG. 3. (a) Top down view of interdigitated electrode sensor and (b) cross-section view of electrode fingers.

the sensor is only 3 cm from the end of one aluminum bond pad to the other, and the sensors measure 0.8 cm wide. The square region of electrode fingers located between the two large bond pads measures 0.8 cm by 0.8 cm. Based on the 0.7 μm finger pitch, this translates into 11 400 fingers, or approximately 92 m of finger length. This large amount of finger length provides a strong capacitance signal and excellent sensitivity to changes in the dielectric properties of the films deposited on top of the electrodes. A 0.8- μm -thick layer of silicon dioxide lies beneath the electrode fingers and serves to isolate the electric fringe fields generated by the fingers from the semiconducting silicon substrate.

C. Capacitance measurements and 248 nm exposures

The presence of photoacid in the PHOST film was monitored by recording the capacitance of the interdigitated electrodes as the exposure dose was slowly increased. All capacitance measurements were performed using a two-point probe station attached to an Agilent model 4284A LCR meter. The two probe tips were applied to the two bond pads located on opposite sides of the electrode finger region, as depicted in Fig. 3. Capacitance values reported in this work were measured at frequencies ranging from 20 Hz up to 100 kHz with an applied bias of 20–50 mV. All 248 nm wavelength exposures were performed using an Oriel Instruments flood exposure source (model No. 87530) equipped with a 248 nm bandpass filter (bandwidth is approximately 11 nm at full width at half max).

D. Resist film optical properties

A variable angle spectroscopic ellipsometer (V-VASE from J. A. Woollam Inc.) was used to measure the optical constants and film thicknesses of the different resist films used in these experiments. For ellipsometry measurements, the materials of interest were cast onto silicon (100) wafers (Nova Electronic Materials). The ellipsometry parameters, Ψ and Δ , were collected over the wavelength range from 200 to 1000 nm at angles of 65°, 70°, and 75°. The Ψ and Δ data were analyzed using the WVASE-32 analysis software (J. A. Woollam Inc.) to obtain film thickness and optical constants by fitting the ellipsometry data using a film stack model composed of a Cauchy layer model for the polymer film, an intervening 15-Å-thick SiO_2 layer, and a semi-infinite silicon substrate layer. The optical constants, n and k , obtained from these measurements were subsequently used in calculations of the exposure intensity profile within the resist film.

III. RESULTS AND DISCUSSION

A. Overview of previous IDE data analysis method

Previously, it was demonstrated that it is possible to utilize capacitance measurements from resist coated interdigitated electrodes to determine the Dill C parameter for a photoacid generator.^{2,3} In order to understand the basis for the new normalization technique discussed in this article, a brief summary of the previously reported Dill C measurement

technique is required. The full discussion of the various aspects of this measurement technique are presented in the previous publications.^{2,3}

The previous technique discussed for measuring the Dill C rate constant based on IDE capacitance requires three basic steps. First, the raw capacitance as a function of exposure dose data is collected. Four to five interdigitated electrodes are spin coated with a thin polymer film loaded with different amounts of a photoacid generator. An initial base line capacitance measurement is taken prior to exposure for the resist film containing only PAG and zero photoproducts. Each of the sensors is then exposed to small increments of UV radiation to decompose a small amount of the PAG and generate photoproducts. A capacitance measurement is taken between each subsequent exposure. Because the dielectric properties of the PAGs photoproducts are somewhat different than the initial PAG molecules', a change in the IDEs measured capacitance occurs. The process of repeating exposures and capacitance measurements continues until no further change in capacitance is observed. This lack of change should indicate that essentially all of the PAG has decomposed into its photoproducts. Figure 4(a) illustrates a typical raw data set collected for a PAG. In this case, triphenylsulfonium triflate was loaded in different amounts into a PHOST matrix and capacitance measurements were recorded at 1 kHz frequency.

The photolysis of a PAG, particularly the onium salt PAGs typically employed in chemically amplified photore-sists, is a complicated, yet well studied phenomenon.^{4–6} A photoacid generator can follow a variety of pathways to produce its photoproducts. For instance, a PAG molecule can receive its energy for excitation via two different mechanisms—direct absorption of a photon or matrix sensitization in which the matrix resin absorbs a photon and passes the energy on to the PAG via electron transfer or some other means. In addition, once the PAG molecule becomes excited it can then proceed down even more reaction pathways depending upon the type of bond cleavage that occurs and whether or not the initial decomposition products become trapped within a solvent cage or manage to escape.

To attempt to model and incorporate each of the various decomposition paths separately into an exposure model for a lithographic simulation would be time consuming and require an extensive amount of experimental work. Furthermore, from a practical point of view, the only piece of information that is typically required is the amount of photoacid produced for a given exposure dose, regardless of the reaction pathways that led to the photoacid generation. Therefore, a far simpler approach is commonly utilized for the purposes of lithography simulation, where a generic first order rate expression is assumed to properly describe the kinetics of PAG decomposition, as shown in Eq. (1):^{7–16}

$$[\text{Photoproduct}(E)] = [\text{PAG}_0](1 - e^{-C \cdot E}). \quad (1)$$

Here $[\text{Photoproduct}(E)]$ refers to the concentration of photoacid, or photoproducts, within the resist film at any exposure dose E , $[\text{PAG}_0]$ refers to the initial concentration of

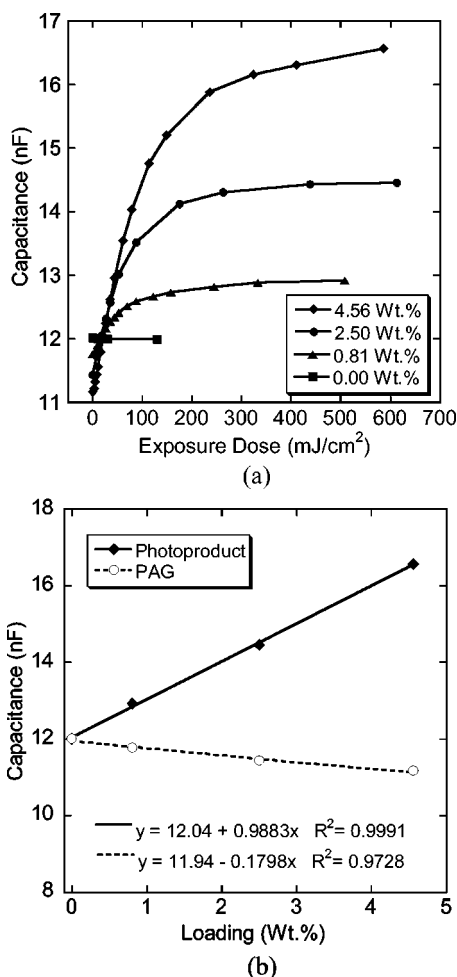


FIG. 4. (a) Capacitance vs exposure dose measured for four different loadings of TPS-Tf PAG in PHOST: ■ 0.00 wt % PAG, ▲ 0.81 wt % PAG, ● 2.50 wt % PAG, and ◆ 4.56 wt % PAG. (b) Linear relationship observed between measured IDE capacitance and PAG/photoproduct loading.

PAG molecules, C is the Dill C first order photolysis rate constant, and E is the exposure dose received by the PAG molecules. It is important to remember at this point that the C parameter takes into account all forms of energy transfer to the PAG, and all potential pathways for PAG decomposition. As a result, the C parameter is not an intrinsic property for a PAG alone, but rather is dependent upon both the PAG and the matrix in which it is being studied.

It is apparent from Eq. (1) that if experimental data regarding the concentrations of PAG and photoproducts versus the exposure dose were available, all that is required to determine the Dill C for the PAG is to fit this equation by adjusting the C parameter to match the experimental data. Thus, the second step in our technique for obtaining the Dill C parameter from the raw capacitance versus exposure dose data is to determine a relationship between measured capacitance and the content of PAG and photoproducts within the resist film.

The key to obtaining this relationship lies within the initial raw data curves that are collected, such as in Fig. 4(a). The initial capacitance measurements are recorded before the

film has been exposed (i.e., an exposure dose of zero) where no photoproducts will have formed in the film and all of the initial PAG molecules are still present. Thus, by examining each IDE capacitance reading at zero exposure dose (with each IDE having been coated with a resist film of varying initial PAG loading), it is possible to obtain a relationship between measured IDE capacitance and PAG content within the resist film. Likewise, the final exposure dose is assumed to correspond to a resist film whose PAG molecules have been fully converted into their photoproducts on a 1:1 molar basis. Thus, by examining each IDE capacitance reading at the final maximum exposure dose, it is possible to obtain a relationship between measured capacitance and photoproduct content within the resist film. Figure 4(b) illustrates such relationships observed for TPS-Tf from the initial raw data displayed in Fig. 4(a).

As can be seen in Fig. 4(b), linear relationships are observed between measured capacitance and both PAG and photoproduct content within the resist film. By combining the two linear relationships observed for PAG and photoproduct capacitance, it is possible to generate a single equation, as shown in Eq. (2), that relates the measured IDE capacitance to the PAG and photoproduct content within the resist film at any given exposure dose E :

$$C_{\text{IDE}}(E) = M \cdot [\text{Photoproduct}(E)] + N \cdot [\text{PAG}(E)] + C_0. \quad (2)$$

In Eq. (2), $C_{\text{IDE}}(E)$ refers to the capacitance measured for the resist coated IDE at any given exposure dose, M refers to the slope of the linear relationship between capacitance and photoproduct content, $[\text{Photoproduct}(E)]$ refers to the concentration of photoproducts within the resist film at a given dose, N refers to the slope of the linear relationship between capacitance and PAG content, $[\text{PAG}(E)]$ refers to the concentration of PAG molecules within the film at a given dose, and C_0 is a constant offset capacitance that corresponds to an IDE coated with a pure PHOST (or other relevant matrix polymer) film with zero PAG or photoproducts present.

Now that a relationship between capacitance and PAG and photoproducts within the resist film has been found, the third and final step is to generate model predicted capacitance versus exposure dose curves to compare to the experimentally obtained curves. First order kinetics, as described by Eq. (1), are used to calculate the concentrations of PAG and photoproducts within the resist film for a given exposure dose and a given value of the Dill C parameter. The capacitance relationship described in Eq. (2) is then used to predict the capacitance that would be measured at the given exposure dose based on the calculated concentrations of PAG and photoproducts within the resist film coated onto the IDE. The model predicted and experimental capacitance versus exposure dose curves are then compared through an appropriate measure of fit, such as the sum of the squared errors (SSE). The Dill C value utilized in Eq. (1) is then adjusted until the fit error between the two curves is minimized. The Dill C that generates the model predicted capacitance curve that best fits the experimental data is then assumed to be the

appropriate Dill C rate constant for properly describing the photolysis kinetics for the PAG being studied.

Again, the previous description of the capacitance measurement technique is somewhat brief, and simplified. Calculations that take into account standing waves, absorbance, and other optical phenomena within the resist film must be performed when calculating the exposure doses that must be used in Eq. (1) for predicting PAG and photoproduct concentrations. In addition, when predicting the IDE capacitance value based on PAG and photoproduct concentrations, the resist film and electrodes must be divided into numerous thin layers in order to account for the various concentration gradients that are formed within the resist film as a result of the standing waves and other optical phenomena. The exposure intensity, concentrations, and resulting capacitance contribution for each slice are calculated and appropriately summed to determine the total measured IDE capacitance for the nominal exposure dose. The details of these calculations can be found in the previous publication on this technique.²

B. Advantages of normalization technique for analyzing IDE data

As can be seen in the previous section, the ability to measure the Dill C parameter depends heavily upon the linear mixing relationship obtained between measured capacitance and the content of PAG and photoproducts within the resist film as described in Eq. (2). This relationship is essentially responsible for permitting generation of the model predicted capacitance versus exposure dose curves for comparison to the experimental data. The quality of this linear mixing relationship obtained for a particular PAG-polymer system has a significant impact upon the accuracy of the measured Dill C value. If the slopes and intercept calculated from the linear fit of the experimental data do not adequately describe all of the experimental data, it is likely that the best fit model capacitance versus dose curve will also fail to capture all of the experimental capacitance versus dose curve data points, resulting in potentially large errors in the calculated Dill C parameter.

Unfortunately, there are many external factors that can influence the base line capacitance of the IDEs and introduce error into the measured linear relationship, especially when measurements on multiple IDE sensors and data collected at different times are involved. For instance, the polymer films typically used for photoresists (such as PHOST) are known to absorb significant quantities of water, and the amount of water absorbed can change considerably as the relative humidity of the ambient environment of the polymer changes.^{17,18} This sorbed water can alter the net dielectric constant of the polymer film resulting in significant changes in the measured capacitance of the resist coated IDE as relative humidity changes.¹⁸ For example, the capacitance of an IDE coated with PHOST (which has been shown capable of absorbing nearly 10 wt % water at 100% relative humidity) has been observed to vary linearly from 9 nF at 0% relative humidity to nearly 16 nF at 100% relative humidity. Thus, the base line capacitance of a resist coated IDE measured at

one time may be different from the base line capacitance measured at a different time for the same identical resist coated IDE simply due to differences in the ambient relative humidity. To combat the problem of shifting IDE base line capacitance with relative humidity, all IDE experiments can be performed in a very short time period on the same day in order to minimize such humidity variations. Nevertheless, the relative humidity in our laboratories has been observed to change by as much as 5% (resulting in a base line capacitance shift of around 0.3 nF for a PHOST coated IDE) during the course of a set of several consecutive Dill C measurement experiments in the worst cases.

In addition to environmental factors such as relative humidity, other factors such as small geometry variations from IDE to IDE can influence the base line capacitance. The IDE sensors utilized in this work were all fabricated at the same time using identical process recipes with the goal of producing sensors that would all be essentially identical. Nevertheless, wafer to wafer, as well as center to edge variations within a wafer can result in small geometric differences from one IDE to another, such as the width of the IDE fingers. At the dimensions at which the IDE sensors used in this work were fabricated, there are over 11 000 fingers used to sense the dielectric properties of the media coating them. Any small change in finger width or height will cause significant changes in the base line capacitance for that IDE sensor. For instance, through the use of conformal mapping equations it is possible to calculate the capacitance measured from an IDE sensor based upon the dimensions of the sensor and the dielectric constants of its materials.¹⁹ Using such equations as described by Hoffman and co-workers, it is possible to simulate the effects of changing the geometry of the finger width and height of the IDE sensors used in this work. The IDE sensors were fabricated using process tolerances of 10%. In other words, the finger height and width could vary $\pm 10\%$ from the target value. If such variations were in fact realized in the IDE sensors, the conformal mapping equations indicate that the base line capacitance of the uncoated IDE in air could vary from 3.89 up to 4.27 nF (actual values measured for the IDEs in this work typically range from near 4.05 up to approximately 4.25 nF). For some PAG/polymer systems, such as TBI-Tf, the magnitude of the capacitance change recorded during photolysis is only on the order of 1 nF using these sensors. Thus, if multiple IDEs with different base line values are utilized to obtain the linear capacitance mixing relationship, significant error could be introduced into the calculated slopes and intercept values for such systems with small capacitance changes.

Figures 5(a) and 5(b) illustrate the type of variation in the linear capacitance relationships that is believed to originate from differences in base line capacitance, either due to humidity changes, IDE geometry differences, or some other factors. The relationship in Fig. 5(a) was observed for data collected from IDEs coated with different loadings of TBI-Tf in PHOST at 1 kHz frequency. Due to the deviations of the experimental data from the best fit line, the slopes calculated from the best fit of the data points in Fig. 5(a) do

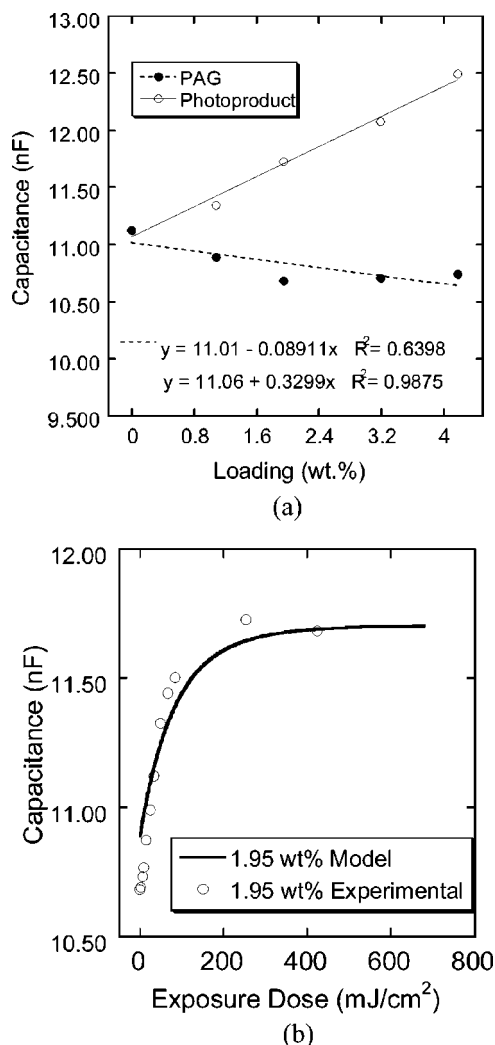


FIG. 5. (a) Linear relationships observed between capacitance and PAG/photoproduct loading for TBI-Tf PAG measured at 1 kHz frequency and (b) best model fit for 1.95 wt % TBI-Tf data.

not allow for a perfect modeling of the capacitance versus exposure dose curve needed to obtain the Dill C. For example, at a loading of 1.95 wt % TBI-Tf, the experimental capacitance for the PAG loaded sample (dose zero) lies well below the best fit line, while the capacitance recorded for the exposed sample (dose final) was well described by the best fit. When the slopes and intercept calculated using the best fit lines of this data are used to create model capacitance curves [such as in Fig. 5(b)], the deviations observed in Fig. 5(a) are transferred into the model fit. The model curve deviates significantly from the experimental data at exposure dose zero and is described quite well at the final dose values. Because of the large deviation at dose zero, the Dill C that provides the best fit of the model to the experimental data will be inaccurate. For this reason, it would be desirable if a means of normalizing the capacitance data could be determined so that variations in base line capacitance due to IDE geometry differences, or other external factors such as relative humidity changes, could be eliminated.

The third, and perhaps most important, reason for deriv-

ing a normalization technique for the capacitance data stems once again from the required linear capacitance versus resist film composition calibration curves described in Eq. (2) and shown in Figs. 4(b) and 5(a). In order to determine this relationship, it is necessary to load known quantities of a desired PAG into the resist matrix. In general, obtaining these calibration data sets is itself a time consuming and material intensive task, requiring the preparation and measurement of a number of different IDE samples. Additionally, if it became necessary to determine the Dill C of an unknown PAG in a resist solution of an unknown composition, there would not be enough information to generate the required linear capacitance versus film composition calibration relationship required by the previous IDE data analysis method. Therefore, a means of normalizing the capacitance data that can eliminate this need for such a capacitance versus composition calibration curve would prove to be invaluable in both saving time and material and by enabling the analysis of “unknown” samples such as commercial photoresist materials.

C. Derivation of a capacitance normalization technique

The normalization technique proposed in this work is based upon the linear relationships between capacitance and PAG and photoproduct content discussed earlier in Eq. (2). This type of relationship has been observed for all PAG-polymer systems studied thus far in our work, and it is assumed for the purposes of this derivation that a similar linear relationship will be observed for essentially all subsequent PAG systems studied. Thus, the derivation of our proposed normalization technique begins with Eq. (2).

As discussed earlier, the relationship shown in Eq. (2) was determined by examining the capacitance values measured on the IDE at the initial and final exposure doses, as depicted in Fig. 6(a). Figure 6(a) displays a typical capacitance versus exposure dose curve generated for a specific loading of PAG in a polymer coated IDE. The initial capacitance value, C_{\min} , corresponds to the capacitance measured for the polymer film at exposure dose zero with all of the PAG molecules initially loaded still present, and zero photoproducts present. The final capacitance value, C_{\max} , corresponds to the capacitance measured for the polymer film at the final exposure dose value once all of the PAG has been converted into its photoproducts. By plotting the C_{\min} and C_{\max} values for this particular loading of PAG, as well as for IDE sensors coated with films containing different amounts of PAG, linear relationships that can be used as capacitance versus concentration calibration curves such as those displayed in Fig. 6(b) are typically observed. In this particular case, it appears that as photoproduct content increases the measured capacitance of the IDE also increases. Likewise, as PAG content of the film increases, the measured capacitance of the IDE decreases. Both linear relationships converge upon a common y intercept, C_0 , that corresponds to the PHOST film with no added PAG or photoproducts. At this time, it is important to point out that these particular slope trends (i.e., PAG content increases, capacitance decreases, photoproduct content in-

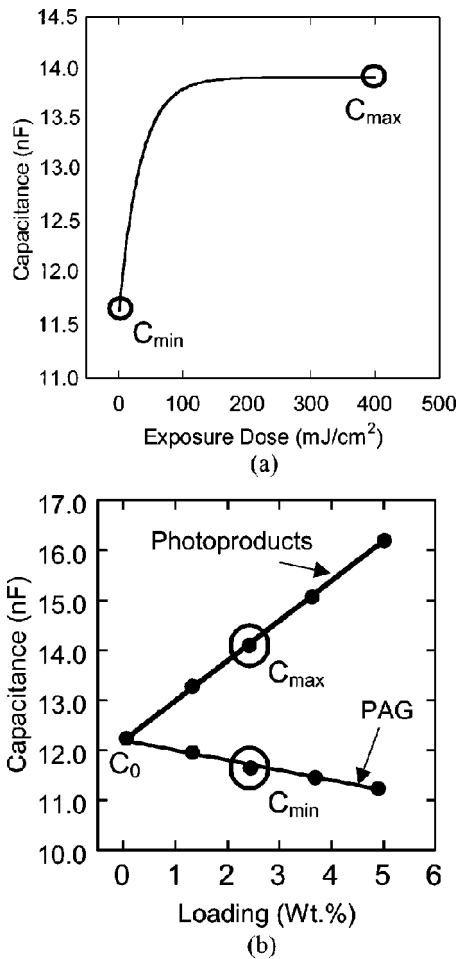


FIG. 6. (a) Typical capacitance vs exposure dose curve generated for a PAG in a polymer matrix. (b) Linear capacitance vs PAG/photoproduct loading in resist film based on raw capacitance data taken from capacitance vs exposure dose curves. The circled data points correspond to the circled data points in Fig. 6(a).

creases, capacitance increases) may not hold true for every PAG that exists due to differences in the dielectric properties from PAG to PAG and their respective photoproduct molecules. For instance, depending upon the PAG and polymer used, the PAG molecules may be more or less polarizable than the pure matrix polymer. As a result, as PAG content increases, the capacitance measured may increase or decrease. Nevertheless, what should be observed in all cases regardless of the PAG and photoproduct's dielectric properties are linear relationships between capacitance and the PAG or photoproduct content. Thus, the measured IDE capacitance can be predicted using an equation such as Eq. (2) with the slopes M and N varying from one PAG system to another depending upon the particular dielectric properties of the PAG.

As just mentioned, Eq. (2) contains two slope values, M and N , that correspond to the slopes of the relationships between measured capacitance, $C_{IDE}(E)$, and the content of photoproducts and PAG, respectively. A closer look at Fig. 6(b) reveals that these two slopes can be written in terms of capacitance values and the concentrations of PAG and pho-

toproducts for the data collected with any given IDE using the simple equation for the slope of a line as follows:

$$\text{slope} = \frac{y_2 - y_1}{x_2 - x_1} \quad M = \frac{C_{\max} - C_0}{[\text{Photoproduct}_{\infty}] - 0},$$

$$N = \frac{C_{\min} - C_0}{[\text{PAG}_0] - 0}. \quad (3)$$

Here C_{\max} and C_{\min} are the capacitance values at the final exposure dose and exposure dose zero for a given loading of PAG and photoproducts as defined earlier, C_0 is the common y intercept at a PAG/photoproduct loading of zero, $[\text{Photoproduct}_{\infty}]$ refers to the loading of photoproducts at the final exposure dose (i.e., where C_{\max} is measured), and $[\text{PAG}_0]$ refers to the initial loading of PAG at exposure dose zero (i.e., where C_{\min} is measured). The slopes M and N are calculated from the slope of a line running from the y intercept at C_0 to the point C_{\max} or C_{\min} . It is important to remember that every raw capacitance versus exposure dose curve collected contains a C_{\max} and C_{\min} value, as well as a $[\text{Photoproduct}_{\infty}]$ and $[\text{PAG}_0]$ value. This stems from the fact that each curve generated is for an IDE coated with a resist film with a different initial loading of PAG.

The term $[\text{Photoproduct}_{\infty}]$ can now be rewritten as $[\text{PAG}_0]$ for the slope M equation if it is assumed that at the final large exposure dose, where C_{\max} is measured, all of the initial PAG molecules have been converted into their photoproducts. Thus, the value of $[\text{Photoproduct}_{\infty}]$ is equal to the value of $[\text{PAG}_0]$. Equation (2) can now be rewritten as the following:

$$C_{IDE}(E) = \frac{C_{\max} - C_0}{[\text{PAG}_0]} \cdot [\text{Photoproduct}(E)] + \frac{C_{\min} - C_0}{[\text{PAG}_0]} \cdot [\text{PAG}(E)] + C_0. \quad (4)$$

As was just mentioned, it is assumed that essentially all of the initial PAG molecules, or $[\text{PAG}_0]$, convert to photoproducts on a one to one molar basis. Thus, the concentration of photoproducts at any exposure dose can be described by the following equations:

$$[\text{Photoproduct}(E)] = [\text{PAG}_0] - [\text{PAG}(E)], \quad (5)$$

$$[\text{PAG}(E)] = [\text{PAG}_0] - [\text{Photoproduct}(E)]. \quad (6)$$

Here $[\text{Photoproduct}(E)]$ is the concentration of photoproducts at a given exposure dose, $[\text{PAG}_0]$ is the initial concentration of PAG molecules, and $[\text{PAG}(E)]$ is the concentration of PAG molecules at a given exposure dose. After substituting Eq. (6) into Eq. (4) and performing some algebraic manipulations, it is possible to derive the following expression:

$$\frac{C_{IDE}(E) - C_{\min}}{C_{\max} - C_{\min}} = \frac{[\text{Photoproduct}(E)]}{[\text{PAG}_0]}. \quad (7)$$

Thus, by inserting expressions for the slopes M and N in Eq. (2), it is possible to show that the raw capacitance data can be normalized into an expression equivalent to the con-

centration of photoproducts at any given exposure dose divided by the initial PAG loading. The raw capacitance values are essentially being normalized against the total change in capacitance that occurs between exposure dose zero and the final exposure dose, or from 100% PAG to 100% photoproducts within the resist film. Recall once again the first order kinetics expression for the decomposition of a PAG into its photoproducts shown earlier in Eq. (1). If the photoproduct concentration in Eq. (1) is normalized against the initial PAG loading, the following simple normalized relationships are obtained:

$$\frac{[\text{Photoproduct}(E)]}{[\text{PAG}_0]} = (1 - e^{-C \cdot E}) = \frac{C_{\text{IDE}}(E) - C_{\text{min}}}{C_{\text{max}} - C_{\text{min}}}, \quad (8)$$

$$(1 - e^{-C \cdot E}) = \frac{C_{\text{IDE}}(E) - C_{\text{min}}}{C_{\text{max}} - C_{\text{min}}}. \quad (9)$$

With Eq. (9), it is now possible to directly compare the raw capacitance data (in normalized form) to the first order kinetics equation. The Dill C parameter can be found by simply computing a curve of the normalized photoproduct value $(1 - e^{-CE})$ versus dose E and adjusting C until this curve best fits the experimentally obtained curve for normalized capacitance versus exposure dose. If a uniform dose of exposure energy were received throughout the resist film that coats the IDE, this calculation would be trivial. Unfortunately, the exposure intensity throughout the film is far from uniform. Optical phenomena such as standing waves and absorbance create complex intensity profiles within the resist film that change in the vertical z direction. Thus, the exposure dose E utilized in Eq. (9) changes from point to point in the z direction. This changing dose means that the normalized concentration of PAG and photoproducts predicted by the expression $(1 - e^{-CE})$ in Eq. (9) also changes in the z direction. To account for these changes, the resist film coating the IDE is divided into thin slices and the exposure intensity along with normalized concentration is then calculated for each thin slice. The normalized concentrations from each slice are then appropriately summed together to determine the overall normalized concentration that would reside within the film coating the IDE for comparison to the normalized capacitance data. The method for calculating the exposure intensities that result from polychromatic standing waves is performed in the same fashion as that described with the previous technique.² In addition, the method used to sum the normalized concentration values from each individual slice is the same as that used to sum the individual slice capacitance values. Each slice's normalized concentration value is multiplied by an appropriate weighting factor depending upon the region of the IDE electric fields from which it originates. Again, the details of this method are also described in the report of the un-normalized technique.²

The advantages of the normalization method presented in this article are numerous. First, variations in sensor to sensor base line capacitance values caused by humidity fluctuations, or from differences in geometry or other electrical properties, are eliminated. The data from each sensor, regardless of base

line capacitance, should always collapse into the normalized relationship described by Eq. (9). More importantly, this technique totally eliminates the need for determining the linear calibration relationship described earlier in Eq. (2) and shown in Figs. 5 and 6. Therefore, it is no longer necessary to coat several IDEs with different loadings of PAG and record capacitance versus exposure dose curves. In theory, it is now possible to coat a single IDE with a resist solution of unknown PAG content and composition and subsequently determine the Dill C parameter from a single capacitance versus exposure dose curve.

D. Application of the normalization technique to previously collected data

In order to test the validity of this normalization technique, the method was used to analyze capacitance data collected from a series of resist coated IDEs. First, the normalization method was used to analyze the capacitance data reported in the previous publication² and the Dill C values obtained from both the original (referred to here as the "original IDE analysis method") and normalization methods were compared. Additionally, several polymer-PAG systems were analyzed using both the original IDE analysis method and the new normalization technique.

Consider first the data previously collected for TPS-Tf in PHOST.² Figure 7(a) illustrates both the model predicted capacitance versus exposure dose curves and the experimental capacitance versus exposure dose curves for loadings of 2.50 and 4.56 wt % TPS-Tf in PHOST. As can be seen, the original IDE data analysis method worked quite well for modeling the capacitance behavior of the TPS-Tf system, producing a Dill C value of 0.044 cm²/mJ for the 4.56 wt % data, and a Dill C of 0.045 cm²/mJ for the 2.50 wt % data, in excellent agreement with C values reported for a similar TPS-Tf/PHOST system by others.^{11,20,21} The model predicted curves and experimental data curves are in excellent agreement. The high quality of fits obtained using the original IDE data analysis method stems directly from the excellent linear relationship obtained for TPS-Tf capacitance versus film composition calibration plot displayed earlier in Fig. 4(b). There is essentially no deviation from the linear fit for any of the data points. Thus, the model predicted curve based upon these relationships should, and does, capture the true behavior very well. Now, consider the same data sets modeled using the normalization approach. Figure 7(b) illustrates the same two data sets analyzed after normalization. Once again, the model predicted curves fit the experimental data curves quite well, this time producing a Dill C value of 0.044 cm²/mJ for the 4.56 wt % data and 0.046 cm²/mJ for the 2.50 wt % data.

Two significant pieces of information are provided by the TPS-Tf data examined before. First, the Dill C values obtained by the original and new normalization methods are in good agreement with one another. This indicates that the normalization based model is predicting the same type of capacitance behavior predicted by the original data analysis method, and thus using the normalized capacitance data in place of the raw, un-normalized capacitance data is accept-

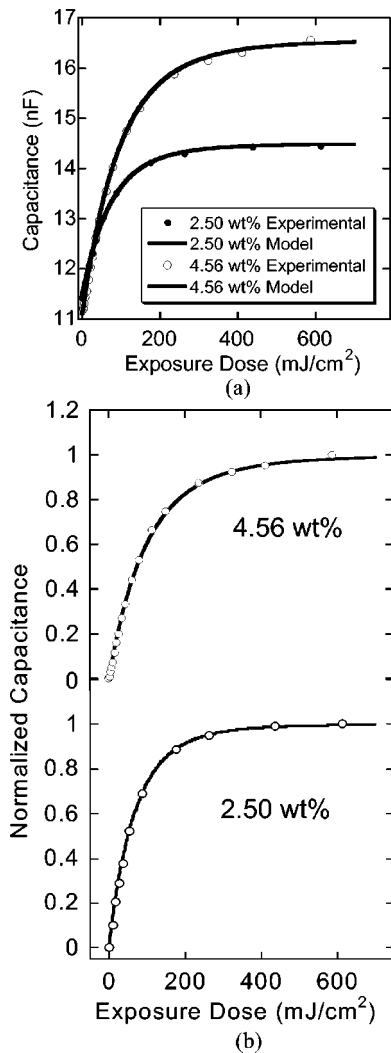


FIG. 7. (a) Comparison of un-normalized model predicted capacitance to experimental capacitance vs exposure dose for TPS-Tf at 1 kHz. (b) Comparison of normalized model predicted capacitance to experimental capacitance vs exposure dose.

able. Second, it is obvious from examining the two figures comparing the model predicted data to the experimental data that there is no significant difference in the quality of the model fits based on the normalized versus the un-normalized model. This again is due to the high quality of the linear relationships obtained between the measured IDE capacitance and PAG and photoproduct content in the TPS-Tf/PHOST system, as illustrated in Fig. 4(b). As can be seen, the linear relationship measured for TPS-Tf predicts the capacitance for all IDEs loaded with different amounts of PAG. Because this relationship already captures the behavior of the IDEs well, with no significant deviations, there is no significant improvement in quality of fit for the model curves generated with the un-normalized method versus the normalized methods.

Now consider data collected for the TBI-Tf PAG in PHOST. The linear relationship between measured IDE capacitance and TBI-Tf/photoproducts concentration, as well as the resulting model fit to the experimental data for a 1.95

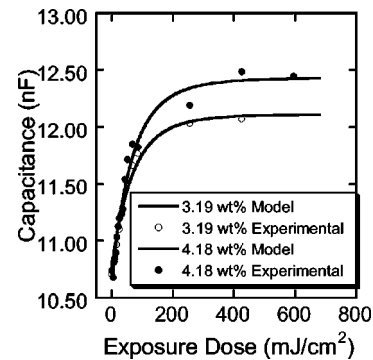


FIG. 8. Un-normalized model predicted capacitance vs exposure dose and experimental capacitance vs exposure dose for 3.19 and 4.18 wt % TBI-Tf at 1 kHz frequency.

wt % loaded sample, were displayed previously in Figs. 5(a) and 5(b). As can be seen, there are small deviations at various points on the curve between the linear model and the experimental data. As a result, when the original IDE data analysis method is used to predict the capacitance versus exposure dose curves, significant deviations occur between the model predicted curve and the experimental curve, particularly at the starting and ending points (dose zero and dose final). Because of the deviations, determining a best fit of the model to the capacitance curve using a quality of fit parameter such as SSE results in less than satisfactory agreement between the model and the experimental data. This in turn results in very little confidence in the Dill C parameters extracted from this data. The use of SSE minimization and other similar fitting techniques result in a Dill C parameter that causes the least deviation from modeled data points to experimental points, regardless of what effect this may have upon the shape of the model predicted capacitance curve. This problem was also displayed earlier in Fig. 5(b). The rate of increase in capacitance versus exposure dose (i.e., the slope of the curve) is different from the experimental data, but this shape is the best fit through the SSE method because the deviations between model data and experimental data are minimized. The best fit Dill C parameter for this data set was found to be 0.041 cm²/mJ using the original IDE analysis method on the raw capacitance data set. Despite the deviations displayed for the data in Fig. 5(b), there were also model predicted curves generated for TBI-Tf in PHOST that did not exhibit such large deviations from the experimental curves. Two such curves are displayed in Fig. 8 for 3.19 and 4.18 wt % TBI-Tf in PHOST measured at 1 kHz. The average best fit Dill C value found for all of the acceptable model fit cases for TBI-Tf was 0.056 cm²/mJ using the original IDE analysis method.

Now, consider the same data set from Figs. 5(b) and 8 with the normalization technique applied. The best fit curves for this data are displayed in Fig. 9. From this figure, it is easy to see that the normalization approach has improved the quality of fit tremendously for the 1.95 wt % data, as indicated by the lack of deviation between model predicted curves and experimental curves. In addition, an average Dill

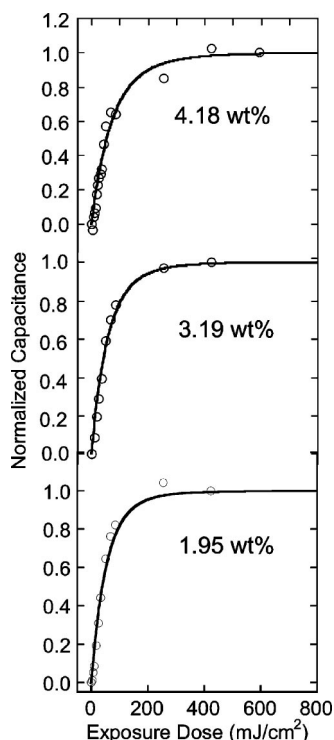


FIG. 9. Normalized model predicted capacitance vs normalized experimental capacitance for 1.95, 3.19, and 4.18 wt % TBI-Tf at 1 kHz.

C of $0.055 \text{ cm}^2/\text{mJ}$ was found using the best fit results of the normalized technique to all of the TBI-Tf data curves collected, in excellent agreement with the average found using the original technique ($0.056 \text{ cm}^2/\text{mJ}$). These values are also in agreement with C values found for TBI-Tf in a PHOST-like matrix using other techniques.^{11,20,21} The ability of the normalization technique to create such excellent fitting curves stems from its derivation from the linear capacitance relationship. Unlike the original IDE analysis method, which relies on experimentally measured values of this relationship, the normalized approach automatically assumes such a relationship exists, without having to actually measure it experimentally. The slope values are automatically lumped into the normalized capacitance. Thus, deviations due to base line fluctuations, etc., are automatically accounted for in the normalized data set.

The specific capacitance curves for TPS-Tf and TBI-Tf discussed in the previous paragraphs were just a few representative examples of how error introduced into the linear mixing relationships can wreak havoc upon the quality of model fits obtained through the original IDE measurement technique. In reality, for each PAG studied, three to four IDEs are each coated with a PAG/polymer sample of different loadings, and then data are collected from each IDE at three to four different measurement frequencies. This means that there are 9–16 raw capacitance versus dose curves collected for each PAG studied. The average of the 9–16 best fit Dill C values is taken and reported as the PAGs Dill C value. The average Dill C values (along with 95% confidence intervals) calculated using the original IDE method and the nor-

TABLE I. Dill C values calculated from both normalized and un-normalized data sets.

PAG	Dill C via un-normalized data (cm^2/mJ)	Dill C via normalized data (cm^2/mJ)
TPS-Tf	0.045 ± 0.0014	0.046 ± 0.0066
TPS-Nf	0.039 ± 0.0075	0.040 ± 0.0021
TBI-Tf	0.056 ± 0.0113	0.055 ± 0.0068
TBI-Nf	0.054 ± 0.0177	0.056 ± 0.0088

malized method on all TBI-Tf curves (not just those shown in the figures in this article), as well as for the TPS-Tf and two other PAGs (TBI-Nf and TPS-Nf) are reported in Table I. To calculate the average values for the “un-normalized data” in Table I, only data from curves demonstrating an acceptable model fit were used. Data from curves showing significant model deviation were omitted from these calculations. From Table I, it is apparent that both techniques predict the same Dill C value within statistical significance, and thus using the normalized capacitance expression to predict the Dill C parameter is an acceptable variation upon the original IDE technique.

IV. CONCLUSIONS

A method has been presented for calculating the Dill C photoreaction rate constant for the generation of photoacid from a photoacid generator in solid polymer films. This method extracts the Dill C parameter using the following assumptions: (1) there is no mechanism for acid loss in the film, (2) first order overall kinetics can be used to describe the process of photoacid generation, (3) the photoacid generator is converted on a 1:1 molar basis to photoacid, and (4) the polymer matrix does not react either photochemically or in the presence of photoacid. Specifically, the method presented here is based on the analysis of normalized capacitance data for photoacid generator loaded polymer films as a function of exposure dose obtained from interdigitated electrode sensors. The normalized data analysis method is a natural extension of the previously demonstrated linear capacitance mixing rules that can be used for describing the dielectric constant of polymer films containing low loadings of photoacid generator.

The use of normalized IDE capacitance data to measure photoacid generator kinetics provides many advantages over the method previously presented for directly using the absolute capacitance data from IDEs to measure the Dill C parameter for PAGs. First, the normalized data eliminates the variations in base line capacitance that can occur due to differences in IDE geometry such as finger width, height, etc. Thus, data can now be collected on IDEs of varying sizes (i.e., without requiring exacting fabrication tolerances for the IDEs) and used universally for measuring photoacid generation kinetics. Second, the normalized approach to measuring the Dill C eliminates the influence of many of the fluctuations in base line capacitance caused by changing environmental conditions such as relative humidity. Thus, data collected from an IDE exposed to 50% relative humidity can

now be compared to data collected at 10% relative humidity without worrying about the changes in base line capacitance that such an environmental difference will cause. It was shown experimentally that the normalized IDE analysis method provides superior model fit quality, and thus in turn can extract more accurate and precise Dill C parameters, in the face of noise and error sources such as varying environmental conditions and natural variations in the size the IDEs used to make such measurements. Finally, and most importantly, the normalized data approach can in theory allow for the characterization of a Dill C parameter for a resist without any prior knowledge of the resist composition or PAG loading. A capacitance versus exposure dose curve generated for a single resist coated IDE, coupled with the resists optical properties, are now sufficient to enable determination of the Dill C parameter for the polymer-PAG system, significantly reducing the amount of time and effort needed to characterize the kinetics of a chemically amplified photoresist.

Additional work is underway to develop experimental methods and analysis techniques that can be used to determine the Dill C parameter for PAGs in solid polymer films under conditions that are less ideal than those specified in this work. For example, methods for addressing the complications induced by photoacid loss have been not been reported in this work. In a true commercial chemically amplified photoresist, base quenchers present within the resist will neutralize photogenerated acid upon exposure and the effects of acid loss due to this phenomenon need to be studied and modeled in order to provide a method that can be robustly used on commercial resist formulations. Additionally, photoresist polymer matrices are designed to be reactive toward photoacid. The effect of such photoacid induced reactions on the ability to use the IDE capacitance methods presented in this work have not been studied in detail at this point. Efforts are underway to study and address both of these issues and the results of this work will be presented in the near future.

ACKNOWLEDGMENTS

The authors would like to thank Dr. Jeffrey Byers of KLA-Tencor Corporation, FINLE Division, and Daniel Miller of SEMATECH for fabricating the interdigitated electrodes used in this work and for their valuable discussions concerning this work. This material is based upon work supported in part by the National Science Foundation through a CAREER award (CLH, Grant No. CTS-9985196).

- ¹L. F. Thompson, C. G. Willson, and M. J. Bowden, *Introduction to Microlithography*, 2nd ed. (American Chemical Society, Washington, DC, 1994), pp. 212–232.
- ²C. Berger and C. Henderson, *J. Electrochem. Soc.* **151**, G119 (2004).
- ³C. Berger and C. Henderson, *Proc. SPIE* **5039**, 322 (2003).
- ⁴J. Crivello and K. Dietliker, *Photoinitiators for Free Radical Cationic & Anionic Photopolymerisation*, 2nd ed. (New York, 1998).
- ⁵J. Dektar and N. Hacker, *J. Am. Chem. Soc.* **112**, 6004 (1990).
- ⁶J. Dektar and N. Hacker, *J. Org. Chem.* **55**, 639 (1990).
- ⁷J. Petersen, C. Mack, J. Thackeray, R. Sinta, T. Fedynshyn, J. Mori, J. Byers, and D. Miller, *Proc. SPIE* **2438**, 153 (1995).
- ⁸A. Pawloski and P. Nealey, *Chem. Mater.* **13**, 4154 (2001).
- ⁹E. Croffie *et al.*, *J. Vac. Sci. Technol. B* **18**, 3340 (2000).
- ¹⁰C. Szmanda, R. Kavanaugh, J. Bohland, J. Cameron, P. Trefonas, and R. Blacksmith, *Proc. SPIE* **3678**, 857 (1999).
- ¹¹C. Szmanda *et al.*, *J. Vac. Sci. Technol. B* **17**, 3356 (1999).
- ¹²J. Cameron, L. Fradkin, K. Moore, and G. Pohlers, *Proc. SPIE* **3999**, 190 (2000).
- ¹³Y. Sohn, H. Oh, and I. An, *J. Vac. Sci. Technol. B* **19**, 2077 (2001).
- ¹⁴A. Sekiguchi, C. Mack, M. Isono, and T. Matsuzawa, *Proc. SPIE* **3678**, 985 (1999).
- ¹⁵D. Ziger, C. Mack, and R. Distasio, *Proc. SPIE* **1466**, 270 (1991).
- ¹⁶N. Jakatdar, J. Bao, C. Spanos, X. Niu, J. Bendik, and S. Hill, *Proc. SPIE* **3677**, 447 (1999).
- ¹⁷C. Berger and C. Henderson, *Polymer* **44**, 2101 (2003).
- ¹⁸C. Berger and C. Henderson, *Proc. SPIE* **5039**, 984 (2003).
- ¹⁹T. Hoffman, K. Schroder, J. Zacheja, and J. Binder, *Sens. Actuators B* **37**, 37 (1996).
- ²⁰A. Pawloski, C. Szmanda, and P. Nealey, *Proc. SPIE* **4345**, 1056 (2001).
- ²¹J. Cameron, N. Chan, K. Moore, and G. Pohlers, *Proc. SPIE* **4345**, 106 (2001).